Chapter 8

Assessing the Performance of Personal Protective Equipment[1]

Georgios Kechagiadakis and Marc Pirlot

Additional information is available at the end of the chapter

http://dx.doi.org/10.5772/65778

Abstract

Lightweight protective structures and materials such as the personal protective equipment (PPE) for explosive ordnance disposal (EOD) personnel are frequently under investigation globally. Their mechanical response to impulsive loads such as blast and ballistic impacts is critical for establishing the spectrum of their performance against various types of threats. This chapter presents a novel testing technique that incorporates three near-simultaneous impacts in one shot in order to acquire deeper understanding of the dynamic interactions that take place during an explosion. A numerical model of an aramid fabric is developed to examine the parameters that influence the ballistic performance under multiple impacts. Fragment cluster impacts with dense dispersion have increased probability to perforate the target material. Heterogeneous, non-isotropic materials, like most of the ballistic grade protective materials, distribute the energy of the impacts in the form of stress wave streams causing the material to behave differently depending on the formation of the impacting fragments. Experimental work with aramid fabrics against single and triple impacts with the fragment-simulating projectile (FSP, 1.102 g) indicates that the ballistic limit in triple impacts is considerably lower that the ballistic limit in single impacts. The actual ballistic performance against multiple fragment impacts is severely underestimated with the classical single-impact methodologies.

Keywords: PPE, fragmentation protection, ballistic test, multiple impacts, triple impacts

[1] "Sometimes I would carry around 100 with me in a sack…"
Aki Ra, Deminer. He cleared 50000 mines
Source: Time magazine

1. Introduction

The deminers are the backbone of mine action. They consider the incidence of accidents during demining operations as low, only once per 25 work years. Most of them have lost family and friends from mine accidents, and in some cases, they have experienced the terrible face of war. An accident is something that happens. But when it happens, the life of the deminer depends on the personal protective equipment, he wears.

The consequences of an accident go beyond the injury of a deminer. Their occurrences affect the morale of the whole demining operation, maiming the motivation of the endeavour. Personal protective equipment serves this way a double purpose. The obligation of the scientific community is to provide with efficient tools to the manufacturers to tune the performance of their products, and clear guidelines to the end users for selecting them.

2. The threat

The physics of anti-personnel (AP) mine explosions may be examined from a science point of view or from a functional point of view. These two perspectives are complementary. The scientific approach aims at describing the details of the fundamental processes that come into play when an AP mine is actuated. This might involve chemistry, physics, material science, etc. The functional approach aims more at the end state, trying to describe the terminal effects of the mine against people and equipment.

All mine explosions share the same fundamental elements: a chemical reaction transforms an explosive material into a hot, high-pressure gas. This gas then performs work, in a thermodynamics sense, on its surroundings. This could be fragmenting the casing of the mine, pushing soil or water, or driving a shock in neighbouring air. It could also be damaging an object or injuring a person nearby. Chemistry and physics provide mathematical equations to describe and quantify these processes. Waves are one of the fundamental quantities in nature. They appear in almost every branch of physics, being associated with light, heat, electromagnetism, etc. In the case of the explosions, the transmission of mechanical waves through a deformable or elastic medium is the most fundamental phenomenon. Such waves originate in the displacement of some portion of an elastic medium from its normal position, causing it to oscillate about an equilibrium position. Because of the elastic properties of the medium, the disturbance is transmitted from one layer to the next. This disturbance, or wave, consequently progresses through the medium. Energy can be transmitted over considerable distances by wave motion. Thus, waves might be construed as being one of nature's mechanisms to transmit and propagate information to materials. Therein lays their importance in describing the physics of mine explosions. This includes the propagation of a detonation wave through the explosive and the subsequent behaviour of the explosive by-products with their surroundings.

When an explosive device detonates, a blast wave is generated, along with multiple accelerating fragments, propagating away to all directions. The blast over-pressure, in extreme

http://dx.doi.org/10.5772/65778

conditions, when it interacts with an individual, may cause amputations and shearing of body parts. It may also cause damage to the ears, which can lead to permanent hearing loss, and due to rapid acceleration to the head, a range of concussive injuries may occur, which can be lethal. The fragmentation of the casing of an explosive device (primary fragmentations), together with dirt, pebbles and debris from the ground (secondary fragmentations), are accelerated by the violently expanding gases of the explosive to supersonic velocities. These fragments, if no adequate ballistic protection is worn, can cause perforations to critical parts of the body resulting to even death.

2.1. Fragmentation mines

Despite significant variations in geometry, mass and materials, all fragmentation mines share the same basic elements and the same working principle. There are four main elements to a fragmentation mine: a main explosive charge, a fragmentation case, a detonator and some actuation (fuse) system. Triggering the fuse usually releases a spring-loaded striker that hits the detonator. The latter is simply a small receptacle that contains a highly sensitive explosive that can be ignited by a simple mechanical hit. This first explosion ramps up to ignite the high explosive that makes up the main charge of the mine. It should be noted that a high explosive is usually much less sensitive than the explosive used in the detonator. This makes it safer to handle and transport the munitions. Detonators are much more sensitive, requiring special packaging and careful handling.

The explosion of the detonator causes the main charge to detonate. As the shock front propagates through the high explosive, it transforms the solid (or liquid) explosive into detonation products. Given that the maximum physical dimension of the main charge for the average fragmentation mine is of the order of 100–200 mm, and assuming an average shock front velocity of 7 km/sec, it takes approximately 15–30 μs to transform the solid explosive into detonation products. In the thermodynamics sense, this mass of hot, high-pressure gas then performs work on its surroundings. For a fragmentation mine, this means breaking up the metallic case into a large number of small fragments and propelling these fragments away from the centre of the explosion at high velocity.

The aim of the fragmentation mines is to cause as many casualties as possible to the opponent, therefore they are extremely dangerous. Current deminer PPE are not able to protect from fragmentation mines.

2.2. Blast mines

An average blast anti-personnel mine contains about 110 g of explosive. The maximum reported charge mass is 300 g and the minimum is 28 g. Blast mines are typically classified in terms of small (less than 50 g explosive), medium (50–100 g of explosive) and large (greater than 100 g of explosive). The most common explosive used in blast mines is Trinitrotoluene (TNT), with Composition B, RDX and other explosives being less common. Most blast mines are concealed in ground.

The vast majority of blast mines are pressure actuated. Two scenarios prevail against this class of mines. In the first scenario, the victim steps on the mine and detonates it as per the intent of the design. In the second scenario, the victim is conducting a mine clearance drill and is in a low-down position when the mine goes off. The main difference between these scenarios is the stand-off distance between the mine and the victim.

A blast mine is a simple device that usually consists of a plastic container filled with the main explosive charge, a detonator and a mechanical actuation (fuse) system. Most detonators rely on stab initiation or a friction sensitive compound to start the combustion process that quickly transitions to a detonation. When a downward force of sufficient magnitude (often less than 10 kg) is applied to the fuse, the mine detonates. It takes between 5 and 10 μs to transform the explosive charge into detonation products. As the detonation wave reaches the mine case, the shock is transmitted to the case, then to the soil and finally, to the sole of footwear or to air. Similar to fragmentation mines, the case breaks up due to the combined effect of the transmitted stress wave and the extreme pressure from the detonation products. However, since the ignition temperature of plastics is much lower than for metals, the case materials also start to combust and continue to do so as they are ejected by the expanding gas. One can surmise that a blast mine relies on three main mechanisms to impart energy to an object nearby. First, it transmits a high-amplitude stress wave into the soil, footwear and air. Secondly, the detonation products expand and perform work on the immediate environment. Thirdly, part of the explosive energy imparts motion to the soil that is then ejected at relatively low velocity (< 1000 m/s) and strikes the victim.

Blast mines are typically used to inflict severe injuries to the enemy unit, causing it to stand in place to attend to the wound. Because of the severity of the injuries, it inflicts a major hit to the morale of the survivors. Current PPE are designed to protect the life of the deminer from all known AP blast mines and reduce the severity of possible injuries.

2.3. Sub-munitions

The term 'sub-munitions' generically describes any item of ordnance carried in or ejected by a dispenser. Anything from a scatterable mine to a remotely delivered radio jammer might be described as a sub-munition, the enormous diversity making it difficult to define their characteristics and effects. A wide variety of launch or delivery system is used, including missiles, rockets, projectiles and mortars. Sub-munitions warheads for these types of land service ammunitions are normally called 'carriers' while bombs containing sub-munitions are generally known as 'cluster bombs'. Some air-delivered sub-munitions are dispensed from canisters that remain attached to the aircraft; examples include the British JP-233, German MW-1 and Russian KMG-U.

Once the dispenser is fired, launched or dropped, opening is normally determined by a time delay or proximity fuse. The sub-munitions are normally dispensed in one of three ways: base ejection, nose ejection or case rupture. Base ejection is most common in projectiles, but is also used in other carriers and some cluster bombs. In both, nose ejection and base ejection, the fuse usually initiates a small propellant charge that opens the carrier and pushes the sub-munitions out. Case rupture, used in some rocket and missile warheads, sometimes involves the use of

http://dx.doi.org/10.5772/65778

small linear cutting charges to split the casing and may also use a propellant charge to eject the sub-munitions. Most (but not all) sub-munitions incorporate a separate arming mechanism (such as wind-driven vanes), which functions, after ejection, as the sub-munition falls. The majority use some form of stabilisation (normally, the fins, a streamer or a chute) to bring them into a nose-down attitude but some are designed to spin in the air stream and use this movement for arming. Since sub-munitions disperse after ejection, the density of the impact footprint is dependent on the speed and altitude at which the dispenser opens. Most sub-munitions are designed to detonate on impact but some (such as scatterable mines) are victim operated or incorporate delays.

3. Current methodologies

Current practices for assessing the performance of PPE have been proven significant for providing basic certified measurements to the humanitarian demining community but they lack physical reasoning. This has led to designs of PPE that over-estimate (expensive and non-ergonomic), or under-estimate the threats deminers are dealing with. The problem of designing PPE is the compromise between adequate protection and comfortability. A better protection is required against various types of threats (splinters, debris, fragments, blast, etc.) but the overall weight and the thermal impact have to remain acceptable for the demining personnel.

Currently, there are mainly two standardised techniques used by the manufacturers to test and certify their products according to the International Mine Action Standards (IMAS) provided by the United Nations Mine Actions Service (UNMAS). Multiple single ballistic impact tests are used to assess the V50, which is the velocity at which there is 50% probability of perforation, in order to test the impact resistance of the PPE against multiple fragment impacts usually generated by an anti-personnel blast-mine explosion event, according to the North Atlantic Treaty Organization (NATO) STANAG 2920. Blast tests are also used to test the structural integrity of the PPE against the blast loads of the explosion. These techniques have helped the humanitarian demining community to understand the necessity of standardised performance and the implementation of validating tools in order to provide the men on the field with certified PPE. However, the above-mentioned techniques have certain limitations. The single impact tests are based on the hypothesis that the effect of a simultaneous multiple-impact event can be simulated with single-impact events, something that is contradictory to the observations on the field. For example, police and armed forces have reported armour system failure when multiple shots impact within certain space and time intervals, called the "double-tap" technique. Also, the blast tests are not that enlightening if expensive measurement devices are not implemented as well, such as biofidelic "crash test" mannequins that cost a few hundreds of thousands of euros. The last point of this critique is that the assumption of analyzing two concurrent phenomena separately, viz. the blast wave over-pressure and the impacts of the fragments, would lead to an accurate and detailed description of the explosion effects, is already a farfetched hypothesis.

4. The triple-impact technique

In 2013, a novel technique for testing protective materials against fragment impacts was presented. Three projectile impacts within close space and time proximity were incorporated in order to simulate the effects of multiple fragment impacts on protective structures. These fragments are typically generated when an explosive device detonates, and they are lethal if no sufficient protection is worn.

4.1. State of the art

The announced ballistic performance of a protective material is highly dependent on the methodology that is followed to assess it [1]. A few attempts have been made to examine the ballistic response of a protective material under near-simultaneous multi-site impacts [2–5]. Qian et al. investigated the terminal effects of fragment cluster impacts on a metallic plate [2,3]. Norris developed a five steel cube launcher for hazard assessments for non-nuclear munitions [3]. Deka et al. developed an air gun triple launcher for conducting near-simultaneous triple-impact tests against S2-glass/epoxy composite laminates [4]. Kechagiadakis et al. examined the response of fragmentation vests against dual impacts from 9 mm to investigate the effect of proximity [6].

After one impact occurs, the material transfers the kinetic energy of the projectile away from the point of impact. The path on which the energy travels depends on the micro- and macro-mechanical structural complexity of the material. Most of the ballistic grade materials are highly complex, heterogeneous and anisotropic. This complexity affects the way the internal stress waves manifest and propagate. Orthotropic materials polarise the three basic (pure) stress waves, the longitudinal and the two shear, on their two main axis of symmetry (for plates) causing the creation of high energy cross-like stress streams[7]. Dynamic interactions of multi-site impacts generate multiple stress wave patterns that superimpose elevating the stress-strain energy density of the material in levels that may decrease its ballistic performance.

Moreover, a target plate after being impacted is beginning to deflect towards the direction of the velocity vector of the impactor till it reaches a maximum. After that point, the transverse wave that caused the deflection is reflected initiating a backwards motion of the plate that begins to oscillate generating Lamb waves. Second and third projectile impacts on an oscillating plate may result to a different terminal effect depending on the phase of this oscillation. A first consequence would be a variant relative velocity the second or third impactor would have with the target plate moving towards or away from the impactor. A second consequence would be the inclination of the deflected plate causing an oblique impact. This effect is more apparent to softer target materials, such as textiles, than metals. For this reason, the present article is focused on the response of aramid fabrics against multiple small size medium velocity impactors.

http://dx.doi.org/10.5772/65778

5. Parameters of the technique

The triple-impact technique is based on the idea that the interactions between multiple impacts influence the ballistic performance of the target material. The complex phenomena that occur during the impact process result in variant responses. These responses are probabilistic, so an enormous number of tests would be required for a sufficiently accurate statistical analysis. Alternatively, with the use of numerical simulations, it is possible to acquire adequate understanding of such a phenomenon. To realise these simulations, a typical aramid fabric is modelled using a homogenised orthotropic elastic shell plate to exhibit the stress wave propagating patterns and three fragment-simulating projectile (FSP) 5.56 mm simple elastic solids are chosen as projectiles [6]. Different configurations of projectile formations with respect to the material's axes of elastic symmetry are modelled in order to acquire a more thorough understanding of the variations in the impact interactions that may be encountered in real ballistic triple impact tests.

The parameters that influence these responses have non-constant weighting factors. There are two major categories of parameters. The ones that have been examined thoroughly in classic ballistics and the ones more related to the interactions of multiple impacts.

Classic ballistics parameters: velocity, projectile shape, impacting materials, obliquity of impact and boundary conditions.

Interactions parameters: projectile formation (dispersion between impacts, rotation of projectile formation, rotation of projectiles and time intervals between impacts) and material directionality (material anisotropy, material heterogeneity and damage propagation). These parameters in most cases are inter-coupling. This means that one parameter influences the weighting factor of another parameter and thus may not be investigated separately.

5.1. Material anisotropy vs. projectile formation

5.1.1. Initial velocity vs. residual velocity

The influence of the projectile formation on the fabric's ballistic response is examined for four cases of triple impacts. The synergistic effects of stress waves and the contact stress concentrations differ from case to case. This differentiation adds further probabilistic properties to the phenomena of terminal ballistics in the cases of multiple impacts. The distance between the projectiles is set to 22.5 mm (**Figure 1**).

5.1.2. Two on-axis impacts and one off-axis impact (case 1)

In this configuration, two of the projectile impacts are aligned with one of the main axis of elastic symmetry of the material. Due to the orthotropic symmetry of the material, the waves exhibit pure longitudinal and shear modes on the main material axes of symmetry and hence they propagate faster. These two impacts interact with each other more intensely than with the third impact because of the constructive/destructive interference their wave stress streams invoke. In this set of simulations, the two on-axis impacting projectiles present generally higher

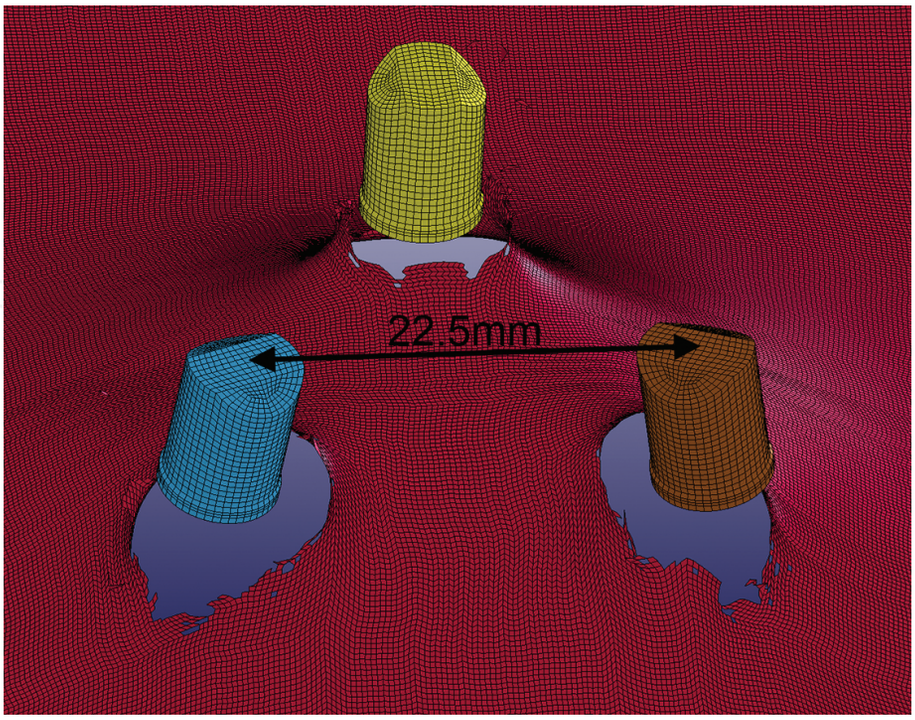

Figure 1. A picture of the parts participating in the simulations.

residual velocities than the third off-axis. Characteristic examples of this phenomenon are the simulations at 420 m/s in which the off-axis impacting projectiles are either blocked or have significantly lower residual velocities (51 m/s).

5.1.3. 15^{O} rotated triple formation (case 2)

Given the orthotropic elasticity of the fabric and the equilateral formation of the three projectiles, there are infinite different rotational configurations that may result in significant deviations of the apparent ballistic performance. However, the rotational ranges in which these configurations may appear in a triple ballistic test are only between 0^{o} and 15^{o}. Beyond the 15^{o}, the line that connects two of the three impact points gradually converges with the second axis of elastic symmetry of the fabric. In this case, the interactions of the three impacts exhibit less dependency on the degree of anisotropy of the fabric.

5.1.4. 90^{O} rotated FSPs (Cases 3 and 4)

The FSPs are projectiles with low length/diameter ratio, resulting in unstable flight after they leave the barrel. Usually, such a problem is minimised by inducing rotational movement on the projectiles, balancing them gyroscopically. While in single-impact tests, this rotational movement induces indifferent ballistic results, in the triple impact case, small deviations may appear. Because of the non-axisymmetrically shaped tip of the FSP, the contact forces that manifest during an impact are not constant along its nose-tip surface. Two areas of stress concentrations appear at the 90^{o} edges of the FSPs tips.

http://dx.doi.org/10.5772/65778

Random rotational orientation of the FSPs result in random stress concentration points on the target and random stress waves source points. Cases 1 and 2 are re-examined for 90° rotated projectiles (**Figure 2**). The resultant residual projectile velocities opposed to the initial velocities for all four cases can be found on (**Figure 3**).

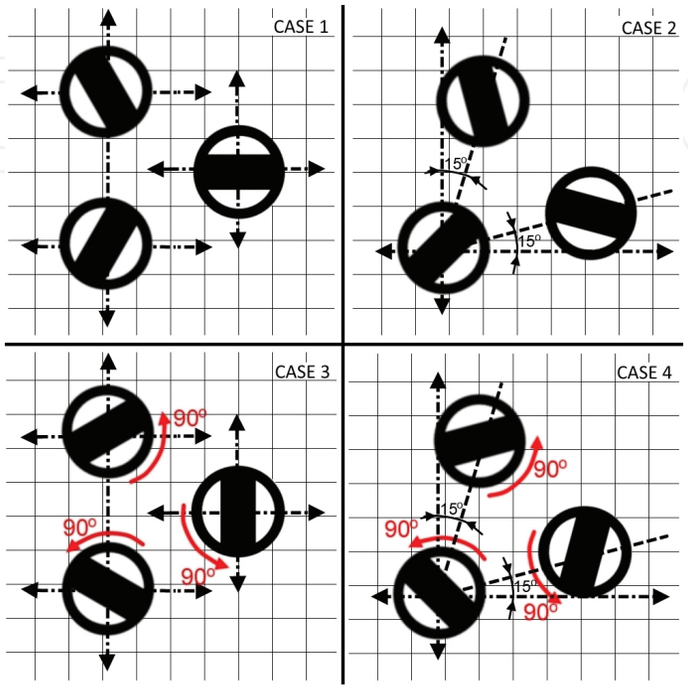

Figure 2. Different triple-impact configurations that were examined. The "dash-dot" axes represent the two axes of elastic symmetry of the material. The black angular increment represents the rotation of the projectile formation around its centre and the red rotational arrows correspond to the rotation of the projectiles around their axial direction.

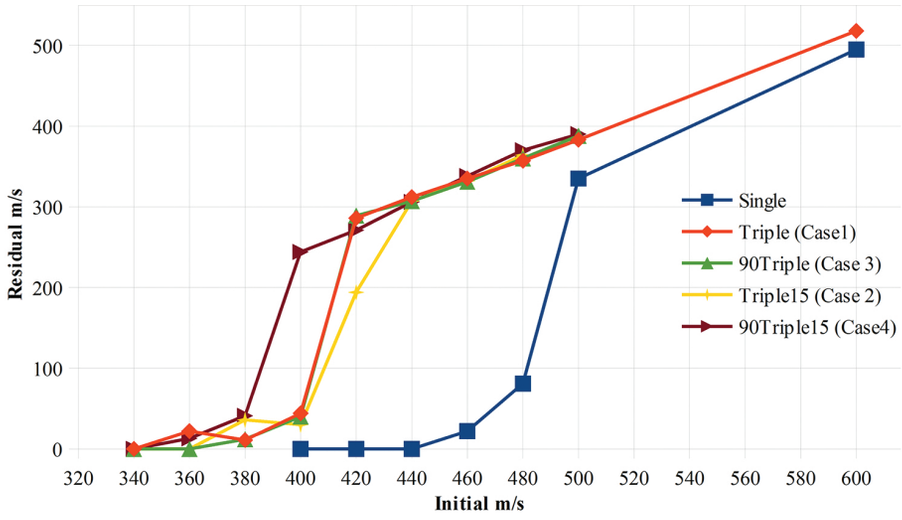

Figure 3. Initial versus residual velocity of single impact and different configurations of triple-impact simulations. The maximum velocities are presented.

5.2. Distinct periods of interactions

The distances between the projectiles, and between the projectiles impact points and the plate's edges were taken into account for calculating the times of arrival of the quasi-longitudinal incident and reflected stress waves. Three distinct periods are observed. In the first period, the projectile has perforated the plate before the stress waves from the other two impacting projectiles reach the point of its impact. The third period is characterised by the influence of the reflected stress waves bouncing at the edges of the plate. The second period is defined between the arrival of the incident and reflected stress waves. In the first period, the projectiles perforate the plate without the influence of multiple-impact interactions due to high initial velocities, over 125% V50. Most cases of multiple plate perforations occur in the second period during which the constructive/destructive interactions coupled with the contact forces and the deflection of the plate have increased probability of failure initiation. In the third, the projectiles have low residual velocities. In **Table 2**, the times of block and initiation of perforation, after contact of the projectiles, are presented.

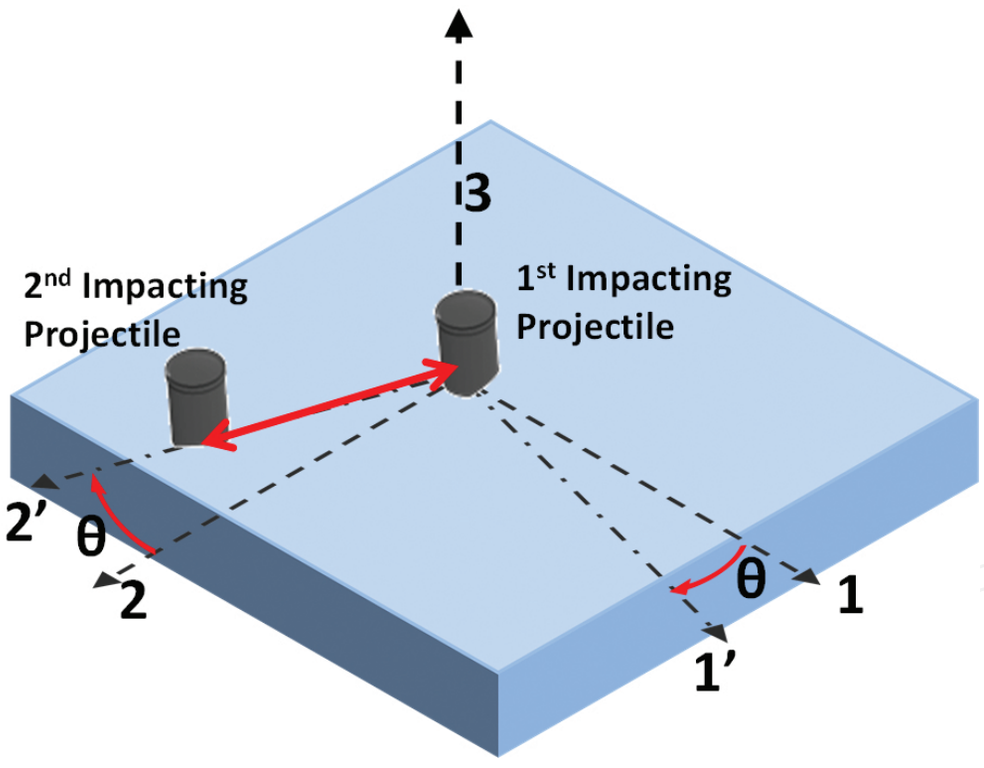

Figure 4. An orthotropic plate being impacted by two projectiles. The axes 1, 2 and 3 represent the axes of material symmetry. The axis that connects impact points of the two impacting projectiles deviates from the axis 2 by θ^{o}.

The times or arrival of stress waves were calculated using the composite material mechanics.

Supposedly, there is an orthotropic plate with axes of material symmetry represented by three dashed arrows 1, 2 and 3 (**Figure 4**). A projectile impacts the plate (at its centre for illustration purposes). Then, another projectile impacts at a second impact point. The line that is defined

http://dx.doi.org/10.5772/65778

by the two impact points defines the path on which the interactions, from and between the two impacts, will occur (marked with red). This line, however, is having an angle in relation to one of the material's axes of symmetry, in this case the second axis.

Then, the stiffness matrix of the plate is [8]

$$\begin{Bmatrix} \sigma_1 \\ \sigma_2 \\ \sigma_3 \\ \sigma_4 \\ \sigma_5 \\ \sigma_6 \end{Bmatrix} = \begin{bmatrix} C_{11} & C_{12} & C_{13} & & & \\ C_{12} & C_{22} & C_{23} & & & \\ C_{13} & C_{23} & C_{33} & & & \\ & & & C_{44} & & \\ & & & & C_{55} & \\ & & & & & C_{66} \end{bmatrix} \begin{Bmatrix} \varepsilon_1 \\ \varepsilon_2 \\ \varepsilon_3 \\ \varepsilon_4 \\ \varepsilon_5 \\ \varepsilon_6 \end{Bmatrix} \tag{1}$$

The material response in directions other than the "on-axis" directions can be calculated by rotating the stiffness matrix, in this case by θ^o.

$$\begin{Bmatrix} \sigma'_1 \\ \sigma'_2 \\ \sigma'_3 \\ \sigma'_4 \\ \sigma'_5 \\ \sigma'_6 \end{Bmatrix} = \begin{bmatrix} C'_{11} & C'_{12} & C'_{13} & & & C'_{16} \\ C'_{12} & C'_{22} & C'_{23} & & & C'_{26} \\ C'_{13} & C'_{23} & C'_{33} & & & C'_{36} \\ & & & C'_{44} & C'_{45} & \\ & & & C'_{45} & C'_{55} & \\ C'_{16} & C'_{26} & C'_{36} & & & C'_{66} \end{bmatrix} \begin{Bmatrix} \varepsilon'_1 \\ \varepsilon'_2 \\ \varepsilon'_3 \\ \varepsilon'_4 \\ \varepsilon'_5 \\ \varepsilon'_6 \end{Bmatrix} \tag{2}$$

This it is possible to calculate the longitudinal stress wave velocities with the formula:

$$V_2 = \left(\frac{C'_{22}}{\rho} \right)^{\frac{1}{2}} \tag{3}$$

where

$$C'_{22} = C_{11}n^4 + 2m^2n^2(C_{12} + 2C_{66}) + C_{22}m^4 \tag{4}$$

$m = \cos(\vartheta)$, $n = \sin(\vartheta)$.

It is possible to draw a curve of the stress wave velocities as a function of degrees (material anisotropy)(**Figure 5**).

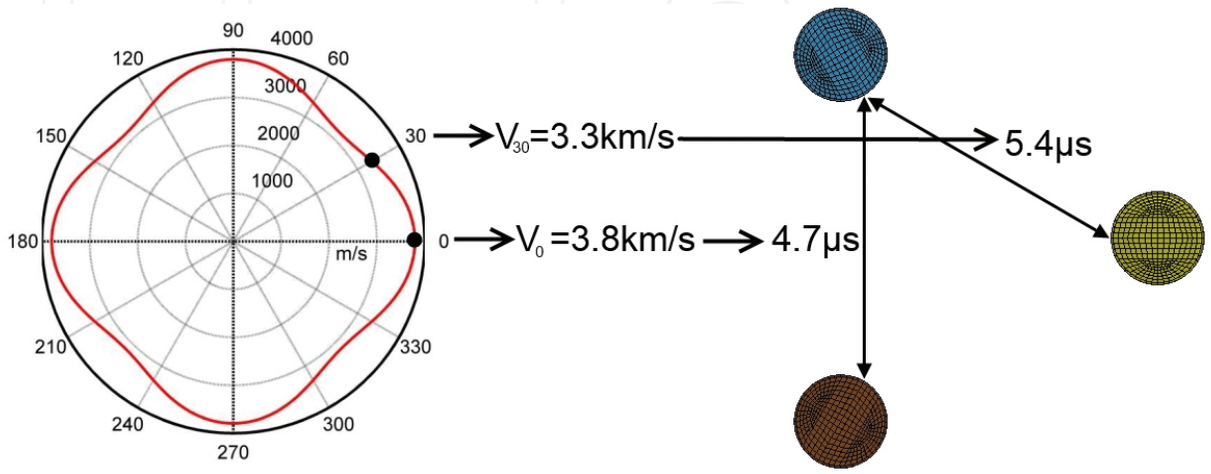

Figure 5. Quasi-longitudinal stress wave velocity as a function of degrees linked to the distances between the projectiles. The times of arrival of the incident waves are calculated.

On the results from the simulations (cases 1-4) are presented (**Table 1**, **Table 2**).

Velocity (m/s)													
Initial	**Single**	**Triple**			**90 Triple**			**Triple 15**			**90 Triple 15**		
340		0	0	0	0	0	0				0	0	0
360		22	0	0	0	0	0	0	0	0	13	0	0
380		11	11	11	12	0	0	36	0	0	41	22	0
400	0	44	34	0	40	29	0	30	10	0	244	32	0
420	0	286	279	51	289	287	0	194	187	32	271	266	80
440	0	312	311	303	307	299	299	307	298	298	306	302	292
460	22	335	328	326	331	330	320	332	331	331	338	326	323
480	81	357	354	354	360	360	351	364	360	354	370	352	351
500	335	383	379	376	388	386	381				390	389	376
600	495	518	517	498									

Table 1. Initial and residual velocities of the projectiles in single- and triple-impact simulations.

http://dx.doi.org/10.5772/65778

Initial velocity	Time of block/perforation (μs)												
	Single	Triple			90 Triple			Triple 15			90 Triple 15		
340		*124*	*126*	*126*	*121*	*123*	*136*				*123*	*123*	*123*
360		*98*	*124*	*125*	*138*	*145*	*188*	*123*	*125*	*125*	*102*	*138*	*172*
380		*97*	*99*	*103*	*98*	*152*	*180*	*97*	*125*	*125*	*97*	*99*	*148*
400	101	*95*	*96*	*128*	*97*	*98*	*122*	*94*	102	*123*	12	*100*	*138*
420	101	9	9	*96*	9	10	*191*	32	34	*94*	9	11	*84*
440	101	9	9	9	9	9	10	9	9	10	9	10	10
460	88	9	9	9	8	8	9	8	8	8	8	8	8
480	76	9	8	8	7	7	8	7	8	8	7	7	8
500	14	7	8	8	7	7	8				6	7	7
600	6	**3**	**4**	6									

Table 2. Time of block (underlined) of the projectiles and time of initiation of erosion of the fabric in single- and triple-impact simulations. With bold are perforations in **Period 1**, with Italic in *Period 3* and normal in Period 2.

5.3. Effect of heterogeneity and anisotropy

Most protective materials apart from their directional composition (anisotropy) have a degree of heterogeneity. This discontinuity within their structure exacerbates the anisotropic distribution of stress waves. As the stress waves propagate inside the material, the internal boundaries between different material segments determine whether the propagation continues or reflects. At the interface between "internal" boundaries within the bulk of the structure, part of the stress waves is transmitted and the rest is reflected depending on the material impedance ratios. The heterogeneity and the anisotropy determine the distribution of the energy of an impact, thus the damage propagating patterns and the interactions between impacts. In the example of the aramid fabric, the stress waves travel within the filaments. Because of their long and thin shape they force the stress waves though the longitudinal direction. The filaments are grouped to yarns. The yarns interchange to form a woven structure. At the contact points between filaments and yarns stress waves are partially reflected and transmitted.

5.4. Effect of dispersion in triple impacts

Dispersion between impacts is an important factor when analysing interactions of multiple impacts. Simulations at three different impact distances were performed in order to define the magnitude of the influence of the dispersion in the ballistic performance of the fabric. The projectile formation was identical to the first case in the triple impacts with two of the projectiles impacting on one of the axes of elastic symmetry of the plate. Simulations with over 420 m/s projectiles initial velocity have shown a decrease of the residual velocity of the projectiles with increasing dispersion. Also, the influence of the orthotropic stress wave polarisation is more intense with the increase of the dispersion. The off-axis impacts have considerably lower "ballistic limit", a phenomenon more apparent in higher ranges of dispersion. The stress wave streams become narrower with increasing radius. The residual projectile velocities as a relation

to the dispersion between the impacts are presented in the (**Figure 6**, **Figure 7**) and on the (**Table 3**, **Table 4**).

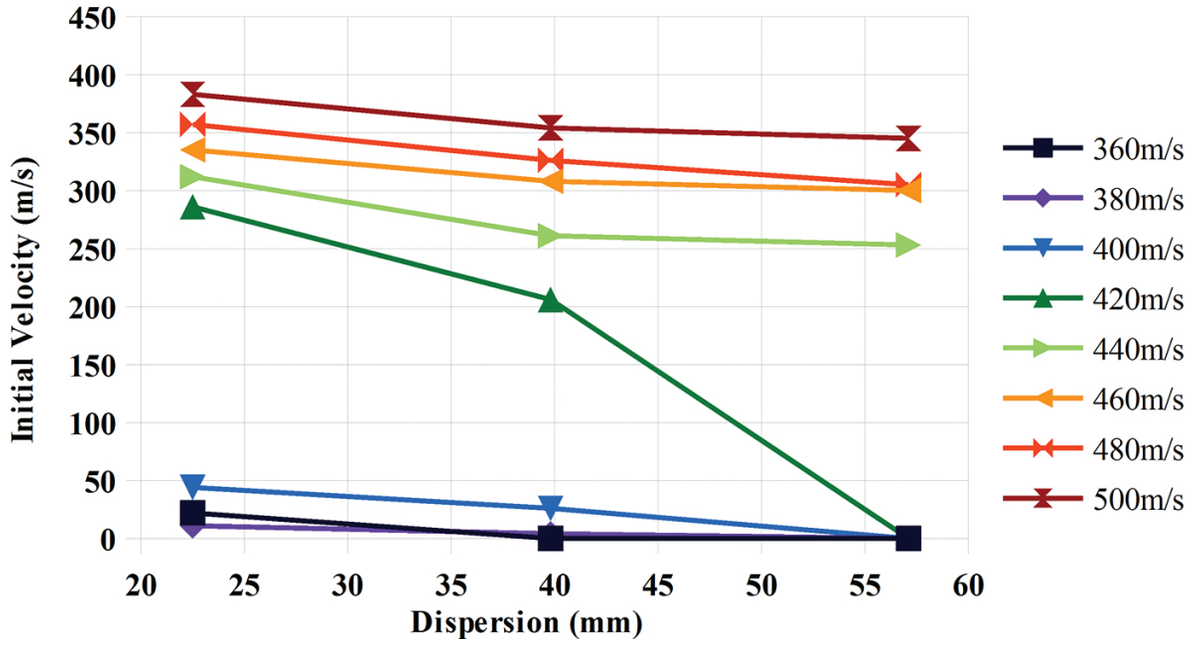

Figure 6. Maximum residual velocity of projectiles in triple impacts as a function of distance between impacts.

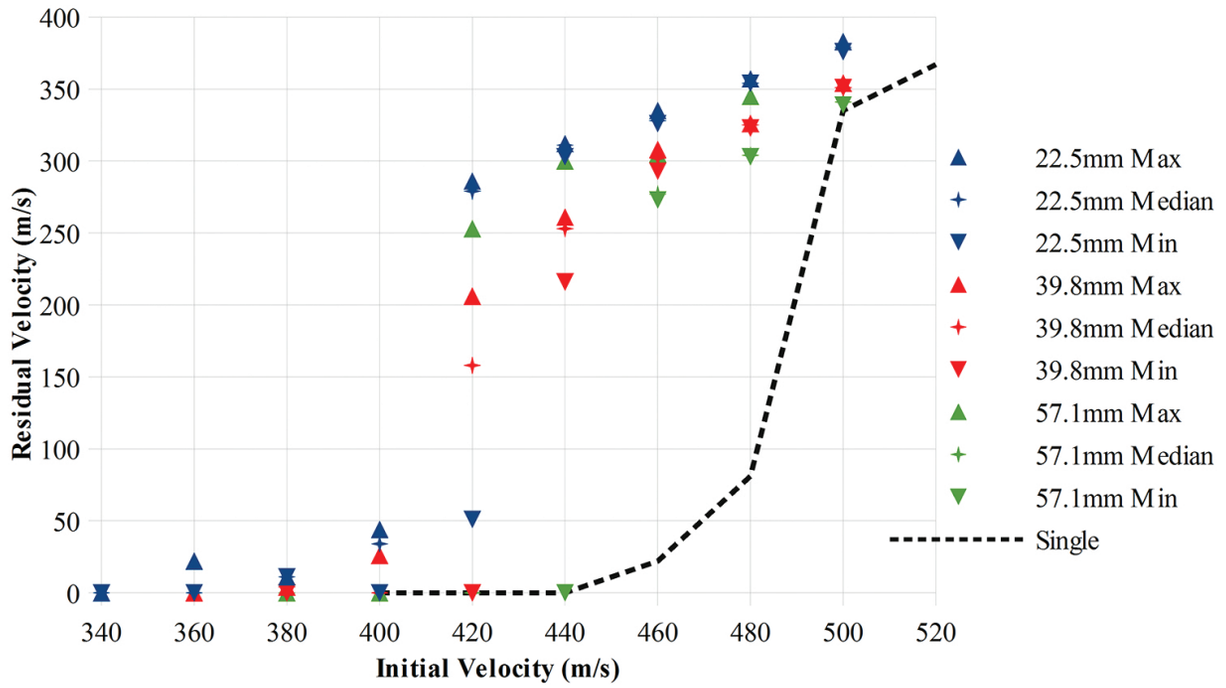

Figure 7. Residual vs initial velocities for three ranges of dispersion.

Velocity (m/s)									
Initial	**22.5 mm**			**39.8 mm**			**57.1 mm**		
340	0	0	0						
360	22	0	0	0	0	0	0	0	0
380	11	11	11	4	4	0	0	0	0
400	44	34	0	26	0	0	0	0	0
420	286	279	51	206	158	0	0	0	0
440	312	311	303	261	253	216	253	253	0
460	335	328	326	308	302	293	300	277	273
480	357	354	354	326	325	323	305	304	303
500	383	379	376	354	351	351	345	341	339

Table 3. Velocities of triple impacts with different radial dispersions.

Initial velocity	Time (μs)								
	22.5 mm			**39.8 mm**			**57.1 mm**		
340	*124*	*126*	*126*						
360	*98*	*124*	*125*	*86*	*89*	*89*	*83*	*83*	*84*
380	*97*	*99*	*103*	*80*	*82*	*87*	*82*	*82*	*84*
400	*95*	*96*	*128*	*75*	*86*	*92*	*81*	*82*	*83*
420	9	9	*96*	24	28	*90*	*80*	*81*	*82*
440	9	9	9	18	19	25	22	22	*92*
460	9	9	9	14	15	15	16	20	21
480	9	8	8	13	13	14	18	18	18
500	*7*	8	8	12	12	13	14	15	16

Table 4. Time of block (underlined) of the projectiles and time of initiation of erosion of the fabric in triple-impact simulations with three levels of projectile dispersion. With Italic in *Period 3* and with normal in Period 2.

5.5. Effect of time interval in multiple impacts

The influence of time and space intervals on the interactions between multiple impacts is direct. As described, the increasing dispersion between impacts results in a gradual convergence with single impacts. The same applies with time. Very long durations between two impacts result in less interactions. The response of the material tends to be indifferent from single impacts. However, a distinction between simple single impacts from single subsequent impacts has to be made. An impact in many cases may cause permanent changes in the target material. Plastic deformation, crack formations and structure distortion are the examples of residual damage from an impact. If the same material is subjected to a subsequent impact (at a different impact point), this residual damage will influence the terminal ballistic response.

The extent of the influence of cumulative damage effects and dynamic interactions in the initiation of perforation in multiple impacts is examined in this section. Four cases of fabrics with pre-defined damage formations are investigated under single and dual ballistic impacts.

The kinetic energy absorption of the fabric is analysed in all four cases and is compared with the single and triple impacts with no pre-defined damaged plates.

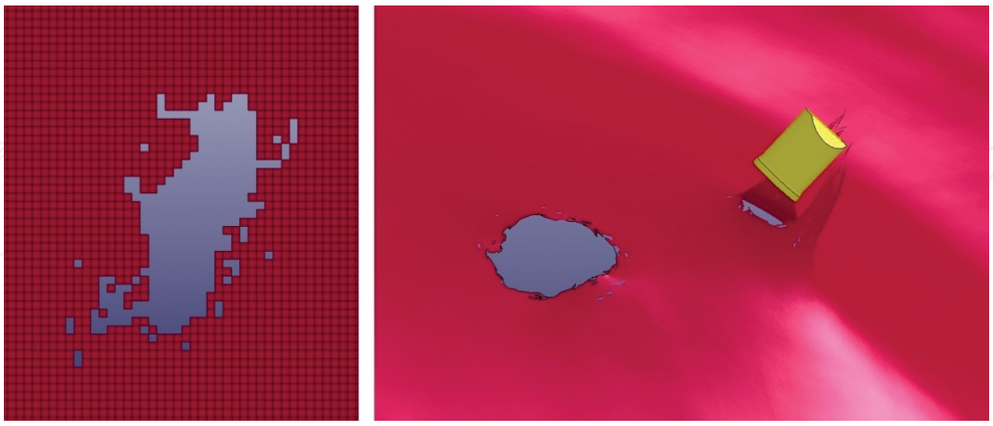

Figure 8. Pre-defined damage pattern, before and during single impact.

The damage patterns that were induced in the plate were taken by the eroded shell elements in the triple-impact simulations at 440 m/s. A small script in Matlab© was written in order to filter and document the eroded elements from the message files from the triple-impact simulations at 440 m/s so to be deleted in the key files. The calculations for the absorbed kinetic energy are based on the difference between the initial/residual velocities of the projectiles. The shapes of the damaged fabrics are presented in the **Figures 8** and **9**. The results are presented in the (**Figure 10**) and on the (**Table 5**).

5.5.1. Fabric with one hole under single impact (cases 5 and 6)

Two simulations with one projectile impacting at two different points of a plate with pre-defined damage were performed. Results show a reduced ballistic performance compared to single-impact simulations on intact plate. More specifically, the energy absorption of the plate was reduced by 4.58–9.37% compared to single-impact simulations and by 37.32–40.46% compared to triple-impact simulations with no pre-defined damage. These results prove the hypothesis that the reduced ballistic performance of the plate is due to the dynamic interactions of multiple impacts. Cumulative damage on the plate during the multiple impacts plays less important role in the initiation or continuation of perforation.

5.5.2. Fabric with one hole under dual impact (case 7)

In this simulation, the cumulative damage effects together with the dynamic interactions of two simultaneous impacts are examined. A pre-defined single perforated plate under dual ballistic impact was performed. The results show elevated energy absorption of the fabric 93.07% more than the single impact with intact plate and 26.83% more than the triple-impact simulations with intact plate. In this simulation, the fabric instead of perforating at the two impact points, the combined impulse from the two projectiles increases the surface tension resulting in shear tearing of the pre-defined hole. Dynamic interactions of the two simultane-

http://dx.doi.org/10.5772/65778

ous impacts seem to increase the energy absorption of the damaged fabric by invoking more extensive damage patterns.

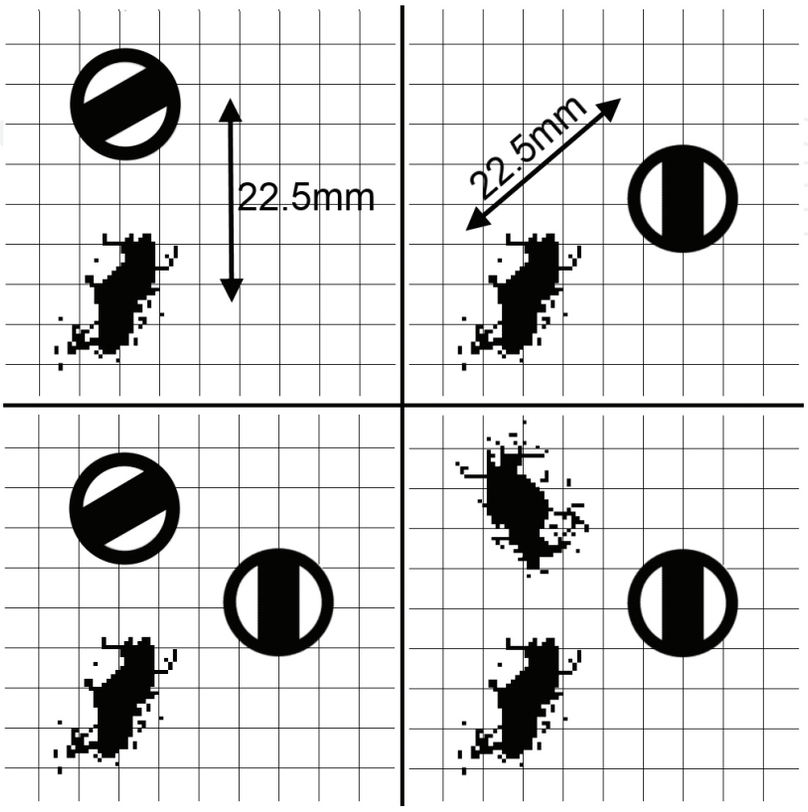

Figure 9. Configurations of simulations with pre-perforated plates.

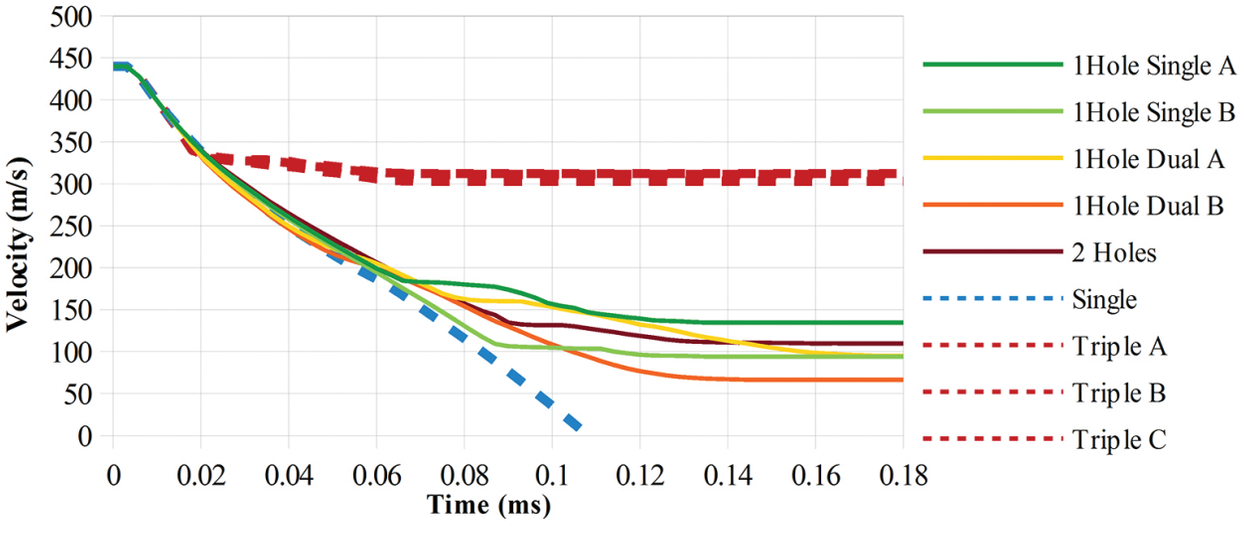

Figure 10. Velocity of projectiles during impact, for single and dual impacts on damaged fabrics and comparison with single and triple impacts on non-damaged fabrics.

Parameter	Effect	Penetrability	Interactions
Velocity	In higher velocities, multiple impacts converge with single impacts. The material responses locally due to inertia. Perforation sequence is fast, thus less interactions are exhibited between multiple impacts.	Increases	Decrease
Projectile sharpness	Sharp impactors induce more localized material responses.	Increases	Decrease
Material hardness	Hard materials respond locally.	Depends on other material properties	Decrease
Obliquity	The impact energy is more distributed.	Decreases	Increase
Boundary conditions	More restricted material response.	Increases	Decrease
Dispersion	In off-axis impacts, the interactions decrease severely with increasing distance. On-axis impacts are less affected.	Decreases	Decrease
Projectile rotation	Flat non-axisymmetric impactors enhance the influence of projectile rotation. The stress concentration points are shifted. Also, anisotropy and heterogeneity exacerbate its influence.	Increases	Depends on anisotropy/ heterogeneity
Formation rotation	Isotropic/homogeneous materials behave indifferently when the formation of the impacting projectiles rotates. Materials with higher degree of anisotropy/ heterogeneity alter their response if the projectile formation rotates.	Depends on Anisotropy/ Heterogeneity	Depends on Anisotropy/ Heterogeneity
Time interval	The time interval between impacts affects other parameters as well, such as the obliquity and the relative impacting velocity. Its effect on penetrability depends greatly on the oscillation phase of the material.	Depends on Phase and/or oscillation phase	Increase generally though some phases are more synergic
Anisotropy	Defines the distribution of stress waves. The material response depends strongly on the formation of the impacting projectiles.	Depends on angle with respect of material axes $f(\theta)$	Depend on angle with respect of material axes $f(\theta)$
Heterogeneity	Defines the distribution of stress waves. The material response depends strongly on the formation of the impacting projectiles.	Depends on coordinates $f(x,y,z)$	Generally decreases Depends on coordinates $f(x,y,z)$

Table 5. Map of the parameters involved in triple impacts.

http://dx.doi.org/10.5772/65778

5.5.3. Fabric with two holes under single impact (case 8)

In this simulation, one projectile impacts on a plate perforated on two points. The same Matlab script was used as with the single-hole simulations without filtering the higher number ID elements. The ballistic performance was in the same levels as with the simulations with a single hole and a single impact with 6.24% absorbed kinetic energy compared to single-impact simulations with no pre-defined damage and 38.41% compared to triple-impact simulations without pre-defined damage.

5.6. Experimental validation of the triple impact technique

A triple launcher was developed for conducting multiple-impact tests on protective structures and materials. The system consists of a 12.7 mm barrel (0.50 in), three 5.56 mm barrels and a custom made diffuser that connects the 12.7 mm barrel to the three 5.56 mm barrels. The whole assembly is fitted on a laboratory universal receiver (**Figure 11**). The triple launcher is capable of shooting three 1.102 g NATO fragment-simulating projectiles (FSP) simultaneously within a range of velocities between 390 and 580 m/s depending on the amount of charge mass that is inserted. The three 5.56 mm barrels are arranged in an equilateral triangular formation.

The charging protocol for the triple launcher is the following:

1. The front piece of the triple launcher, which holds the three 5.56 mm barrels, is removed in order to have access to the chambers of the 5.56 mm barrels.
2. The three 1.102 g FSP are loaded in the three 5.56 mm barrels.
3. The front piece is reattached to the rest of the assembly.
4. The 12.7 mm barrel is then loaded with a cartridge containing the desired amount of combustion powder.
5. The weapon system is armed and ready to shoot.

After ignition, the combustion gases are directed from the 12.7 mm barrel to the diffuser. The diffuser redirects the gases through the 5.56 mm barrels accelerating the three 1.102 g FSP.

The triple-impact technique was evaluated experimentally against 15 layers of plain weave Kevlar® K29. The fabrics were fully clamped on a 100 x 100 mm clamping device and they were tested against single and triple impacts of 1.102 g FSP (**Figure 12**). The single-impact tests were conducted with the use of a standard single barrel of 5.7 mm and the triple-impact tests with the triple launcher. In total, 10 fabrics were tested against single shots and eight against triple shots. The velocities were measured using a Photron high-speed camera that was positioned laterally, filming perpendicular to the projectiles flight. A second high-speed camera was also used to monitor the status of the material during impact and to assist evaluating which of the shots was perforating (in the case of triple impacts).

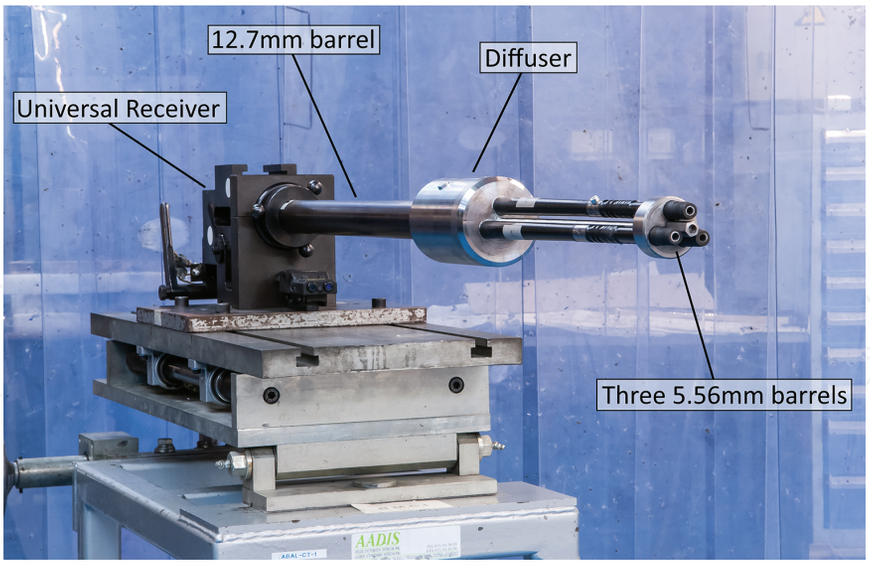

Figure 11. The triple launcher.

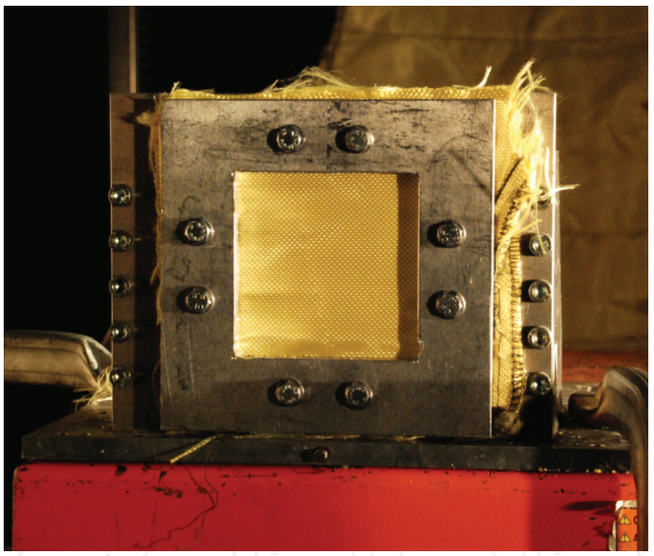

Figure 12. Clamped 15 layers of Kevlar® K29.

The experimental results for the single-impact tests were processed using the Probit calculation method and the results were fitted with the normal cumulative distribution. For the triple-impact tests, the results were calculated as an average velocity value per triple shot. The results from the triple-impact tests were fitted with the Weibull cumulative distribution using the method of least squares. The ballistic limit of the aramid fabric in single-impact tests was 455 m/s while based on the triple-impact tests, the ballistic limit dropped to 426 m/s (**Figure 13**). The terminal ballistic results can be found on the (**Table 6**). Seven consequent instances of a triple impact test, with three FSP being ejected towards an aramid specimen can be found on the (**Figure 14**).

Test	Velocity/average velocity (m/s)	P/NP	V50 (m/s)
Single	433	NP	
Single	438	NP	
Single	449	NP	
Single	451	P	
Single	453	NP	**455**
Single	459	P	
Single	465	P	
Single	465	NP	
Single	466	P	
Single	467	P	
Triple	349	NP	
Triple	419	NP	
Triple	421	3P	
Triple	428	NP	**426**
Triple	430	1P	
Triple	433	NP	
Triple	434	3P	
Triple	435	2P	

Table 6. Results from tests single versus triple impacts.

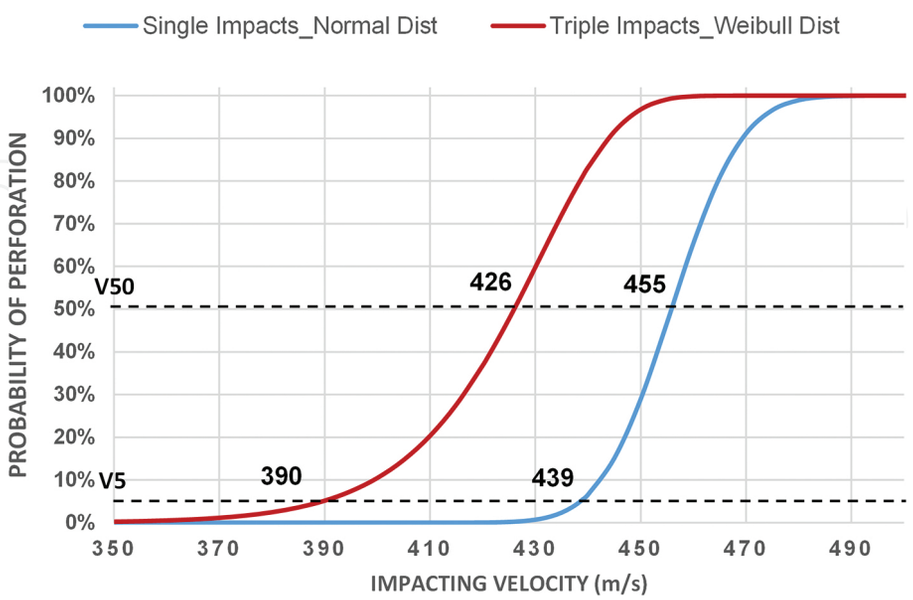

Figure 13. Probability of perforation as a function of impacting velocity for single and triple impacts.

The probability density function that is produced reveals the true value of the triple-impact technique. The V50 is a statistical value that has not direct practical use. The velocity at which perforation is improbable, i.e. 5%, is more usefull for the end users and the manufacturers. Due to the unpredictable nature of the interactions between multiple impacts, the actual difference of the ballistic performance may be much greater.

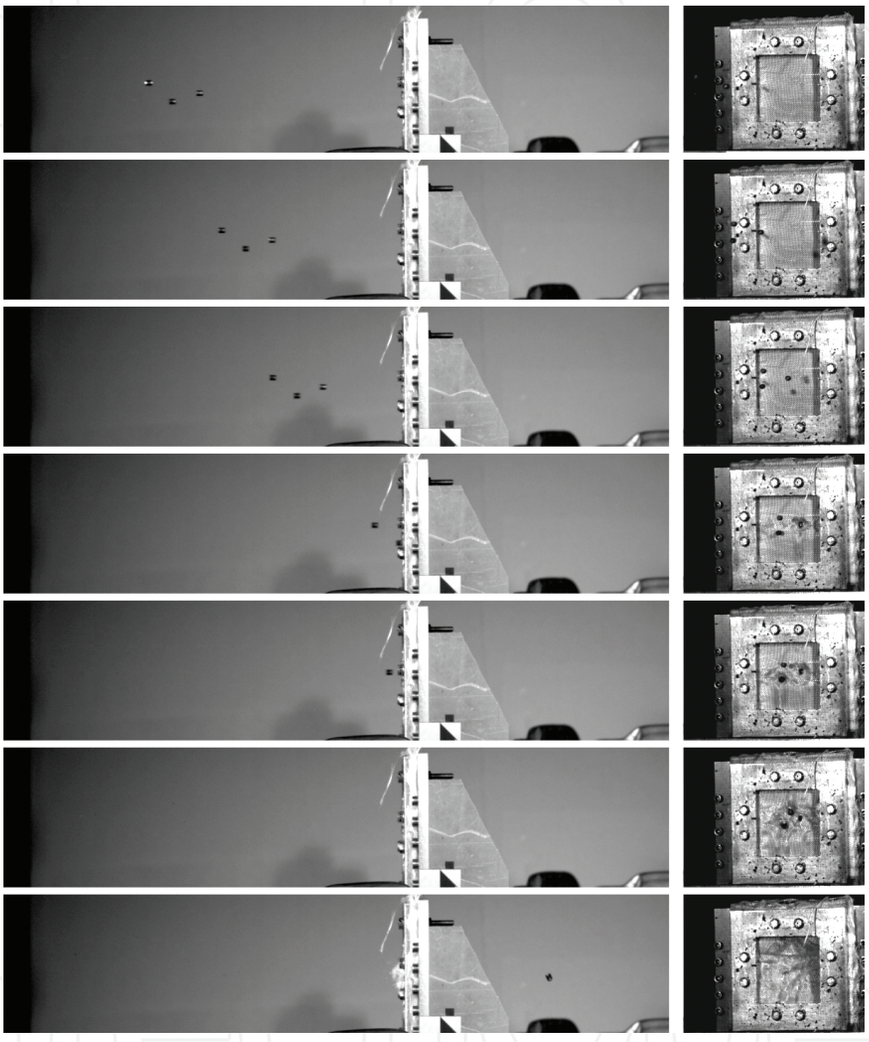

Figure 14. A triple impact test that resulted in single perforation.

6. Conclusions

- Numerical simulations and experimental results have shown a significant decrease of the ballistic performance of the aramid fabric under triple impacts compared to single impacts. The constructive/destructive interference of the stress wave patterns of the three impacts increase the stress-strain energy density of the material closer to its strength.

- Different configurations of triple impacts, such as the orientations of the projectile formation, the rotation of the projectiles (in the case they are not axisymmetric) and their radial dispersion, and modify the material's apparent ballistic performance.
- With the increase of the initial velocity of the triple impacts, their residual velocity converges with the residual velocity of the single impacts.
- The on-axis impacts due to generation of pure mode longitudinal stress waves interact more intensely and exhibit higher residual velocities.
- With increasing distance between the projectiles, the triple impact interactions decrease; thus the penetrability tends to converge with the one in single impacts.
- With increasing distance between the projectiles, the influence of paired on-axis impacts becomes more obvious. This happens because of the stress wave streams that become narrower in higher distances. Non-pure (quasi-longitudinal) waves become evanescent.
- The ballistic performance in simultaneous multiple impacts cannot be assessed with subsequent impacts.
- The existence of damage on the target material does not imply necessarily reduction of the ballistic performance.

Acknowledgements

The research leading to these results has received funding from the European Community's Seventh Framework Programme (FP7/2007–2013) under grant agreement number 284747 (TIRAMISU project).

Author details

Georgios Kechagiadakis* and Marc Pirlot

*Address all correspondence to: georgios.kechagiadakis@rma.ac.be

Royal Military Academy, Brussels, Belgium

References

[1] Roey J.V, Rabet L, Reck B, Bousu F, Imad A. Experimental investigation of the failure of fabric armour during ballistic impact. Proceedings of the 2nd International

Conference of Engineering against Fracture (ICEAF II); June 2011; Mykonos, Greece; p.22—24.

[2] Qian L, Qu M, Feng G. Study on terminal effects of dense fragment cluster impact on armor plate. Part I: Analytical model. International Journal of Impact Engineering; 31; 2005; 755–767.

[3] Qian L, Qu M. Study on terminal effects of dense fragment cluster impact on armor plate. Part II: Numerical simulations. International Journal of Impact Engineering; 31; 2005; 769–780.

[4] Norris FE. Description of the five steel cube launcher used in the multiple fragment impact test. Naval Air Warfare Center Weapons Division China Lake, CA, No. NAWC-WPNS-TP-8062. June 1993.

[5] Deka L.J, Bartus S.D, Vaidya U.K. Multi-site impact response of S2-glass/epoxy composite laminates. Composites Science and Technology; 69; 2009; 725–735.

[6] Kechagiadakis G, Pirlot M, Doucet A. The material response of PPE against Dual Impacts: The Double Tap. Proceedings of the 12th International Symposium "Mine Action 2015"; 27–30 April 2015; Biograd, Croatia; ISSN 1849-3718; p. 67–71.

[7] Nayfeh A.H. Wave propagation in layered anisotropic media with applications to composites. North-Holland Series in Applied Mathematics and Mechanics; 39; 1995; 31–115.

[8] Jones R.M. Mechanics of Composite Materials. Technology and Engineering; CRC Press; 1 July 1998; p. 55–66 ISBN 9781560327127.